A modified formulation of fractional stratiform condensation rate in the NCAR Community Atmospheric Model (CAM2)

Minghua Zhang and Wuyin Lin
Institute for Terrestrial and Planetary Atmospheres, State University of New York, Stony Brook, New York, USA

Christopher S. Bretherton
Department of Atmospheric Sciences, University of Washington, Seattle, Washington, USA

James J. Hack and Phillip J. Rasch
National Center for Atmospheric Research, Boulder, Colorado, USA

Received 9 May 2002; revised 23 August 2002; accepted 30 August 2002; published 15 January 2003.

[1] This paper describes a modified formulation of stratiform condensation rate associated with fractional cloudiness in the Community Atmospheric Model Version 2 (CAM2). It introduces an equation to link cloudiness change with the variation of total condensate. Together with a diagnostic cloud relationship that represents subgrid-scale variability of relative humidity, a closed system is formed to calculate the fractional condensation rate. As a result, the new formulation eliminates the two closure assumptions in the *Rasch and Kristjànsson* [1998] prognostic cloud scheme. It also extends the *Sundqvist* [1978] scheme by including the influence of convective detrainment and advection of condensates on the fractional cloudiness. Comparison is made between the present formulation and the Rasch and Kristjànsson scheme by using data from the Atmospheric Radiation Measurement Program and through global model simulations with CAM2. It is shown that relative to the Rasch and Kristjànsson scheme, the new formulation produces less clouds and a slightly warmer troposphere, thus reducing the original cold bias in the National Center for Atmospheric Research (NCAR) Community Climate Model (CCM). Even though the overall impact of the new formulation on the model climate is small, the modifications lead to more consistent treatments of fractional cloudiness change, condensation rate, and cloud water change in the model. *INDEX TERMS:* 0320 Atmospheric Composition and Structure: Cloud physics and chemistry; 3319 Meteorology and Atmospheric Dynamics: General circulation; 3337 Meteorology and Atmospheric Dynamics: Numerical modeling and data assimilation; *KEYWORDS:* fractional condensation, cloud scheme, Community Atmospheric Model (CAM)

Citation: Zhang, M., W. Lin, C. Bretherton, J. Hack, and P. J. Rasch, A modified formulation of fractional stratiform condensation rate in the NCAR Community Atmospheric Model (CAM2), *J. Geophys. Res.*, *108*(D1), 4035, doi:10.1029/2002JD002523, 2003.

1. Introduction

[2] Parameterization of clouds in climate models has been the subject of active research in the last twenty years [*Sundqvist*, 1978; *Slingo*, 1987; *Le Treut and Li*, 1988; *Smith*, 1990; *Ghan and Easter*, 1992; *Tiedtke*, 1993; *Del Genio et al.*, 1996; *Fowler et al.*, 1996; *Rasch and Kristjànsson*, 1998]. This is primarily motivated by the importance of potential cloud radiative feedbacks on climate change [e.g., *Somerville and Remer*, 1984; *Cess et al.*, 1990; *Mitchell and Ingram*, 1992]. It is widely recognized that uncertainties in cloud parameterizations are still the main cause of discrepancies in the 1.5 to 4.5 degree global warming simulated in general circulation models (GCM) from a doubling of CO2 concentration in the atmosphere [*Cubasch et al.*, 2001].

0148-0227/03/2002JD002523$09.00

[3] Two lines of complication arise in the parameterization of clouds in large-scale models. One is from the spatial and temporal subgrid-scale variability of the dynamic, thermodynamic, and hydrological variables within a GCM grid box. The second is from microphysical processes associated with the size distribution of cloud condensation nuclei and hydrometers. The first aspect is ideally dealt with by using high-resolution models, while the second aspect requires spectrally resolved descriptions of cloud particles. The two aspects, unfortunately, interact with each other, and they also interact with the resolved-scale atmospheric circulation. Even with the rapid pace of improvement of computing power, it is impossible to resolve the important subgrid structure and the spectral information of clouds in the foreseeable future for global climate model simulations. As a consequence, simple subgrid-scale models and aggregated spectral hydrometer information are still needed to parameterize clouds.

[4] One of the subgrid-scale issues of cloud parameterization is the calculation of fractional condensation rate, which is directly related with the calculations of fractional cloudiness and local cloud microphysical processes. In CCM2, condensation rate is calculated based on grid-scale saturation, and temperature and water vapor mixing ratio are correspondingly updated. Fractional cloudiness and cloud water were diagnosed separately from the condensation rate. As a result, time variation of cloud water may be inconsistent with the condensation rate. Later versions of the CCM3 used the *Rasch and Kristjànsson* [1998] (hereafter referred to as RK98) prognostic cloud scheme, in which condensation rate is used to update the temperature, water vapor, and cloud water. The condensation rate, however, was calculated based on two closure assumptions, and cloudiness change was not directly linked with cloud water change. Because of these assumptions, the in-cloud condensate, which was diagnosed from the updated cloudiness and the total cloud water, was not constrained and may not be consistent with the cloud water equation for the cloudy portion of the grid box. Another line of prognostic cloud schemes following *Sundqvist* [1978] (hereinafter referred to as S78) used one closure assumption to calculate the fractional condensation rate, which is then used to update temperature, water vapor, cloudiness, and total cloud water. As in RK98, the in-cloud condensate was diagnosed rather than being governed by its own controlling equation.

[5] The present study reformulates the RK98 scheme to start from an in-cloud condensate equation. Total cloud water variation is then expressed in terms of changes of cloudiness and in-cloud condensate. Together with a diagnostic cloud relationship, a closed set of equations is formed to derive the fractional condensate rate. As a result, our formulation eliminates the two closure assumptions used in RK98 and the one closure assumption used in S78. This modification of linking cloudiness change with cloud water also allows the inclusion of cloud water advection and detrainment in the calculation of fractional cloudiness.

[6] The paper starts with the description of the proposed formulation and its implementation in CAM2. Comparison is made in section 3 with other schemes. Section 4 first shows results from diagnostic and single column model calculations using field observations from the Atmospheric Radiation Measurement program (ARM) and then results from GCM simulations. The last section summarizes the findings.

2. Formulation

2.1. Governing Equations

[7] As in S78 and RK98, the controlling equations of water vapor mixing ratio, temperature, and total cloud water, are written as

$$\frac{\partial q}{\partial t} = A_q - Q + E_r \tag{1}$$

$$\frac{\partial T}{\partial t} = A_T + \frac{L}{C_p}(Q - E_r) \tag{2}$$

$$\frac{\partial l}{\partial t} = A_l + Q - R_l, \tag{3}$$

where A_q, A_T, and A_l are tendencies of water vapor, temperature, and cloud water from processes other than large-scale condensation and evaporation of cloud and rain water. A_q, A_T and A_l include advective, expansion, radiative, turbulent, and convective tendencies, which may consist of evaporation of convective cloud water and convective rainwater. For simplicity, we call them advective tendencies. For now, they are uniformly applied to the whole model grid cell; this assumption has some conceptual shortcomings and an alternative is discussed in section 2.4. Q is the grid-averaged net stratiform condensation of cloud water (condensation minus evaporation). This definition differs slightly from RK98 who used it for condensation only; it also differs from S78 who used it to include evaporation from both cloud water and rain/snow water. The reason for this distinction will become clear later. E_r is the grid-averaged evaporation rate of rain/snow water. R_l is the conversion rate of cloud water to rain/snow water.

[8] Similar to S78, the controlling equation of relative humidity of U, when written on a pressure surface, can be derived from equations (1) and (2) as

$$\frac{\partial U}{\partial t} = \alpha\frac{\partial q}{\partial t} - \beta\frac{\partial T}{\partial t} = \alpha A_q - \beta A_T - \gamma(Q - E_r), \tag{4}$$

where

$$\alpha = \frac{1}{q_s}, \quad \beta = \frac{q\,\partial q_s}{q_s^2\,\partial T}, \quad \gamma = \alpha + \frac{L}{C_p}\beta.$$

α, β, and γ are all positive. They can be viewed as efficiencies of moisture advection, cold advection, and net evaporation in changing the relative humidity U, thus potentially the fractional cloud cover. As in S78 and RK98, ice saturation is not separately considered here; rather, it is approximated by a weighted average $q_s(T)$ of the saturation mixing ratios over ice and water (the dependence of q_s on pressure is not made explicit since pressure enters into our calculation only as a parameter).

[9] All the above equations are applicable on both grid and subgrid scales as long as Q, E_r and R_l are correspondingly defined. In the following, we use a hat to denote variables in the cloudy portion of a grid box to distinguish them from variables of the whole grid box, and we use a to denote the fractional cloud coverage. For the portion of the grid box that is cloudy before and after the calculation of fractional condensation (i.e., the cloudy area that does not experience clear-cloudy conversion), equation (4) becomes

$$\alpha\hat{A}_q - \hat{\beta}\hat{A}_T - \hat{\gamma}\hat{Q} = 0.$$

Thus the condensation rate in this portion of the grid box is

$$\hat{Q} = \frac{\alpha\hat{A}_q - \hat{\beta}\hat{A}_T}{\hat{\gamma}}, \tag{5}$$

and the in-cloud condensate equation becomes

$$\frac{\partial \hat{l}}{\partial t} = \hat{A}_l + \frac{\alpha\hat{A}_q - \hat{\beta}\hat{A}_T}{\hat{\gamma}} - \hat{R}_l. \tag{6}$$

Since the total cloud water can be written as $l = \hat{l}$, one has

$$\frac{\partial l}{\partial t} = a\frac{\partial \hat{l}}{\partial t} + \hat{l}^*\frac{\partial a}{\partial t}. \tag{7}$$

We use $\hat{l}^*$ to denote the mean cloud water of the newly formed or dissipated clouds within a time step as an attempt to crudely describe some subgrid information of cloud water. The first term on the right-hand side of the above equation represents cloud water change of existing clouds, the second term represents cloud water change associated with expansion and contraction of cloud boundaries. Theoretically, newly formed or dissipated clouds should have zero cloud water content. Practically, however, because of the finite time step in the integration of the cloud water equation, the second term may be relevant. In fact, RK98 took $\hat{l}^* = \hat{l}$. Substituting the above into equation (3), using equation (6), $R_l = a\hat{R}_l$ and as well as $A_T = \hat{A}_T$, $A_q = \hat{A}_q$, $A_l = \hat{A}_l$ one has:

$$\hat{l}^*\frac{\partial a}{\partial t} = (1-a)A_l + Q - a\left(\frac{\alpha A_q - \hat{\beta}A_T}{\hat{\gamma}}\right). \tag{8}$$

This equation states that the condensation rate is linked with fractional cloudiness change as required by the total water budget. As long as Q can be calculated to integrate equations (1)–(3), it can be also used to integrate equation (8) to predict cloudiness changes. The definition of Q to include both condensation and evaporation of cloud water is therefore the most convenient in the present formulation. If $\hat{l}^*$ is set to be zero in equation (8), the condensation rate Q can be directly derived from equation (8). The scheme then becomes extremely simplified.

[10] Note that we do not have a true prognostic equation for cloudiness as given by *Tiedtke* [1993] and *Randall and Fowler* [2001]. We therefore cannot explicitly consider advection of cloud volume and detrainment of cloud mass from convection. Equation (8), however, attempts to describe these processes by using the source of cloud water (A_l) divided by the in-cloud water. This feature is lacking in the RK98 and S78 schemes. Equation (8) is not integrated in the present formulation. Instead, it is used to calculate the condensation rate described as follow.

2.2. Subgrid-Scale Assumption

[11] Following RK98, we use the CCM diagnostic fractional cloud scheme as our subgrid-scale assumption. Namely, fractional cloud cover and grid-scale relative humidity are related as

$$a = a(U, b), \tag{9}$$

where b denotes a generic variable describing vertical stability, local Richardson number, cumulus mass flux etc. b changes with space and time. This equation is assumed to be valid when the relative humidity U is larger than a threshold value U_{00}, which is the minimum grid-scale relative humidity with clouds.

[12] Taking partial derivative of the above equation with respect to time, one has

$$\frac{\partial a}{\partial t} = \frac{\partial a}{\partial U}\frac{\partial U}{\partial t} + \left(\frac{\partial a}{\partial b}\right)\frac{\partial b}{\partial t}.$$

After defining

$$F_a = \frac{\partial a}{\partial U}, \text{ and } F_b = \left[\left(\frac{\partial a}{\partial b}\right)\Big/\left(\frac{\partial a}{\partial U}\right)\right]\frac{\partial b}{\partial t},$$

we have

$$F_a^{-1}\frac{\partial a}{\partial t} = \frac{\partial U}{\partial t} + F_b. \tag{10}$$

We assume that F_a and F_b can be calculated without the knowledge of the condensation rate. Substituting the relative humidity equation (4) into the above equation, one has

$$F_a^{-1}\frac{\partial a}{\partial t} = \alpha A_q - \beta A_T - \gamma(Q - E_r) + F_b. \tag{11}$$

Eliminating $\frac{\partial a}{\partial t}$ between equations (8) and (11), one can derive

$$Q = c_q A_q - c_T A_T - c_l A_l + c_r E_r + \sigma\hat{l}^* F_b, \tag{12}$$

with

$$c_q = \frac{\alpha}{\hat{\gamma}}a + \left(1 - \frac{\gamma}{\hat{\gamma}}a\right)\sigma\alpha\hat{l}^*$$

$$c_T = \frac{\hat{\beta}}{\hat{\gamma}}a + (1 - \frac{\gamma}{\hat{\gamma}}\frac{\hat{\beta}}{\beta}a)\sigma\beta\hat{l}^*$$

$$c_l = (1-a)\sigma F_a^{-1}$$

$$c_r = \sigma\gamma\hat{l}^*,$$

where

$$\sigma = \frac{1}{F_a^{-1} + \gamma\hat{l}^*}.$$

All coefficient variables are nondimensional except for C_T and β with a unit of 1/K. All are positive. Once Q is obtained, equations (1)–(3) and (8) can be integrated. In practice, equation (9) can be used to update cloudiness.

[13] Physical interpretation of equation (12), which is valid when $U \geq U_{00}$, is as follows: moist advection (positive A_q) and cold advection (negative A_T) produce condensation. Evaporation of rain/snow water (positive E_r) also produces cloud condensation, because it changes the mean relative humidity, thus increasing cloud amount and cloud water. Import of cloud water (positive A_l) leads to evaporation. This is less intuitive: it increases cloud fraction, thus requiring a higher clear-sky relative humidity, which has to be generated by evaporation. The increase of cloud fraction from a nonwater source through F_b, however, requires condensation.

[14] The prognostic cloud equation can be written as

$$\left[F_a^{-1} + \gamma\hat{l}^*\right]\frac{\partial a}{\partial t} = \left(1 - \frac{\gamma}{\hat{\gamma}}a\right)\alpha A_q - \left(1 - \frac{\gamma}{\hat{\gamma}}\frac{\hat{\beta}}{\beta}a\right)\beta A_T$$

$$+ (1-a)\gamma A_l + \gamma E_r + F_b, \tag{13}$$

which can be obtained by either substituting equation (12) into equation (8) or by eliminating Q between equations (11) and (8). Moist advection (positive A_q), cold advection (negative A_T), evaporation of rain/snow water (positive E_r), and import of cloud water (positive A_l) all lead to an increase of cloud amount.

[15] We note that the closure to constrain the calculation of Q is not restricted to equation (10). Suppose one can predict information on the subgrid-scale distribution of T and q with given Q (say gravity waves, convection plumes, or simply linear functional fitting using neighboring grids), or probability distributions of total water and liquid water temperature [*Le Treut and Li*, 1988; *Smith*, 1990], fractional cloud cover can be then derived and used with equation (8) to constrain the calculation of Q.

[16] In the work by *Smith* [1990], where a triangular distribution of total water is assumed and its standard deviation is dependent on the grid saturation mixing ratio, he derived an explicit relationship between grid-scale fractional cloudiness and mean relative humidity as *Smith* [1990, Appendix C]:

$$a = 1 - \left[\frac{3}{\sqrt{2}}\left(\frac{1-U}{1-U_{00}}\right)\right]^{\frac{2}{3}}.$$

In S78, and similarly, in the works of *Sundqvist et al.* [1989], *Del Genio et al.* [1996], and *Zhao et al.* [1997], equation (9) is assumed to follow $U = aU_s + (1 - a)U_0$ where $U_s(=1)$ is the cloudy sky relative humidity and U_0 is the clear sky relative humidity written as a linear function of the total cloud cover $U_0 = (1 - \mathrm{a})U_{00} + a$. U_{00} is a constant, taken as 75% in S78. This relationship between U and a can be derived from a top-hat distribution of the total water content within a grid cell.

2.3. Implementation in CAM2

[17] The diagnostic cloud scheme of *Kiehl et al.* [1996] and RK98 is used as equation (9). To evaluate F_a, the cloud routine is called twice each time step with relative humidity perturbed by one percent while holding all other variables in the model fixed. Thus

$$F_a = \frac{\Delta a}{\Delta U} = \frac{a^* - a}{U^* - U}.$$

We assume that all b variables are fixed in the stratiform condensation calculation, thus $F_b = 0$. We also assume a top-hat distribution of the cloud water distribution as in S78 and RK97, thus $\hat{l}^* = \hat{l}$. The entire microphysical package of RK98 is used for: (1) the partition of l into cloud liquid and cloud ice with a prescribed temperature dependent factor, (2) the calculation of cloud-to-rain/snow conversion rate of $R_l = a\hat{R}_l$, which includes cloud liquid water autoconversion to rain, the collection of cloud water by rain and snow, the autoconversion of cloud ice to snow, and collection of ice by snow, (3) the calculation of rain and snow using R_l integrated from above, (4) evaporation of rain and snow, which is used as E_r.

[18] With equation (12), input variables of the scheme are: T, q, p, A_T, A_q, A_l, a, l, $F(a)$; E_r is diagnostically calculated as a function of these input variables. Output variables are Q, R_l, updated T, q, l, a, and microphysical conversion rates.

[19] The impact of convection on cloud cover can be implemented straightforwardly. Detrainment of cloud water from the *Zhang and McFarlane* [1995] convection scheme is used as input in the calculation of A_l, so is the impact of convection on A_T and A_q. The detrained cloud water from convection was originally assumed to evaporate in the Zhang and McFarlane scheme. This is also the treatment in the original Arakawa-Schubert scheme [*Arakawa and Schubert*, 1974]. This portion of the water is now made available to the stratiform clouds for possible evaporation and precipitation. A more rigorous treatment will require the subgrid-scale partition of the detrained water and coupled convective-stratiform interactions, a subject pursued by *Randall and Fowler* [2001]. Note that in RK98, detrainment of cloud water only affects the condensate budget; while in the present formulation, it also affects the cloudiness and stratiform condensation rate.

[20] Because of the finite time step, in the implementation, the calculation is carried out by categorizing each model grid into one of the four scenarios: (1) whole grid saturation with $U = 1$, Q calculated from equation (5); (2) $1 > U \geq U_{00}$, Q calculated from equation (12); (3) $U < U_{00}$ but $l > 0$, Q calculated as $-l$; (4) $U < U_{00}$ and $l = 0$, $Q = 0$. The use of the threshold relative humidity is a result of the assumption of equation (9).

2.4. An Alternative Formulation Using Total Water and Liquid Water Temperature

[21] The above derivation assumed uniform tendencies of A_T, A_q, A_l across the cloudy and clear portions of the grid. This assumption can be relaxed. Within the clear part of the grid box, the noncondensational liquid water tendency A_l is not physically meaningful. More fundamentally, an implicit assumption of the RK98 approach is that the cloudy and clear air within the grid box are advecting together. Physically, if we neglect virtual effects, this requires that the cloudy and clear air maintain the same temperature, and hence the same temperature tendency. However, the condensational tendency of temperature will be different in the cloudy air than in the clear air, so to compensate, the noncondensational temperature tendency also must be different in the cloudy than in the clear air, in contradiction to the assumption of RK98 and section 2.1.

[22] In this section, we present a reformulation of the approach of section 2.1 using thermodynamic variables conserved during phase changes of water. We use the total specific humidity (vapor plus condensate) $r = q + l$ and liquid water temperature $T_l = \mathrm{T} - (L/C_p)l$ for our formulation. Instead of assuming A_T, A_q, A_l all uniform, we assume: (1) that the temperature of the cloudy and clear air are equal, and (2) that the total water tendency of $A_r = A_q + A_l$ is uniform across the grid box.

[23] The governing equations of total water r and liquid water temperature T_l can be written from equations (1)–(3) as

$$\frac{\partial r}{\partial t} = A_r + E_r - R_l \tag{14}$$

$$\frac{\partial T_l}{\partial t} = A_{T_l} + \frac{L}{C_p}(R_l - E_r), \tag{15}$$

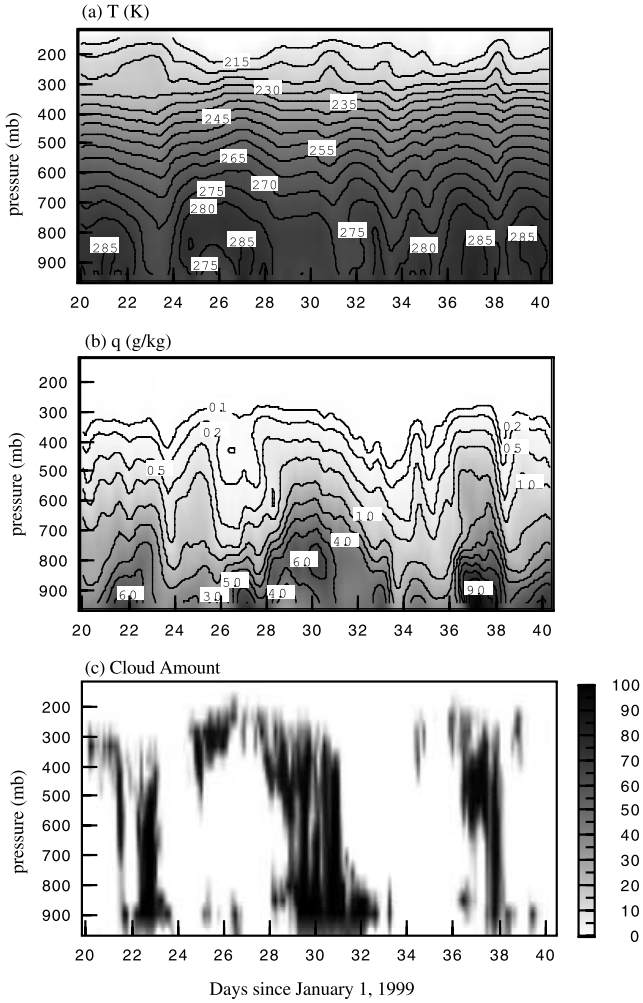

Figure 1. Time-height distribution of measurements from the ARM SGP winter 1999 IOP. (a) Temperature, (b) water vapor mixing ratio, (c) cloud frequency derived at the SGP central facility.

where $A_r = A_q + A_l$ and $A_{T_l} = A_T - \frac{L}{C_p}A_l$. A relative humidity equation similar to equation (4) can be derived by noting $U = q/q_s = [r - l]/q_s(T_l + Ll/C_p)$, so

$$\frac{\partial U}{\partial t} = \alpha\frac{\partial(r-l)}{\partial t} - \beta\frac{\partial\left(T_l + Ll/C_p\right)}{\partial t} = \alpha\frac{\partial r}{\partial t} - \beta\frac{\partial T_l}{\partial t} - \gamma\frac{\partial l}{\partial t}. \quad (16)$$

For the cloudy portion of grid, $\hat{U} = 1$, so that $\frac{\partial\hat{U}}{\partial t} = 0$. Hence we can apply equation (16) to the cloudy portion only to obtain

$$\hat{\gamma}\frac{\partial\hat{l}}{\partial t} = \alpha\frac{\partial\hat{r}}{\partial t} - \hat{\beta}\frac{\partial\hat{T}_l}{\partial t} = \alpha\frac{\partial\hat{r}}{\partial t} - \hat{\beta}\frac{\partial\left(\hat{T} - L\hat{l}/C_p\right)}{\partial t}.$$

It can be shown that the tendency of in-cloud condensate from the above equation is the same as in equation (6). Now we diverge from section 2.1 by introducing the assumption that the cloud and clear-air temperatures remain equal, so $\hat{T} = T$. With $\alpha = \hat{\gamma} - \hat{\beta}L/C_p$, the above equation then becomes

$$\alpha\frac{\partial\hat{l}}{\partial t} = \alpha\frac{\partial\hat{r}}{\partial t} - \hat{\beta}\frac{\partial T}{\partial t} = \alpha\frac{\partial\hat{r}}{\partial t} - \hat{\beta}\frac{\partial\left(T_l + Ll/C_p\right)}{\partial t}$$
$$= \alpha\frac{\partial\hat{r}}{\partial t} - \hat{\beta}\frac{\partial T_l}{\partial t} - \frac{L\hat{\beta}\partial l}{C_p\partial t}.$$

Substituting equation (7) into the above, noting that $\frac{\hat{\beta}}{\alpha} = q_s' = \frac{\partial q_s}{\partial T}$ one has

$$\left(1 + a\frac{Lq_s'}{C_p}\right)\frac{\partial\hat{l}}{\partial t} = \frac{\partial\hat{r}}{\partial t} - q_s'\frac{\partial T_l}{\partial t} - \frac{Lq_s'\hat{l}^*}{C_p}\frac{\partial a}{\partial t}. \quad (17)$$

Unlike the corresponding equation (6), this equation does not contain the noncondensational temperature tendency for the cloudy portion of the grid box.

[24] If $\hat{l}^*$ is set to be zero, equations (17) and (7), together with equations (14) and (15), form a closed set of equations. With other choices of $\hat{l}^*$, as in RK98, the system can be closed by substituting equation (16) into (10), and using equation (7) to obtain

$$F_a^{-1}\frac{\partial a}{\partial t} = \alpha\frac{\partial r}{\partial t} - \beta\frac{\partial T_l}{\partial t} - \gamma\left(a\frac{\partial\hat{l}}{\partial t} + \hat{l}^*\frac{\partial a}{\partial t}\right) + F_b. \quad (18)$$

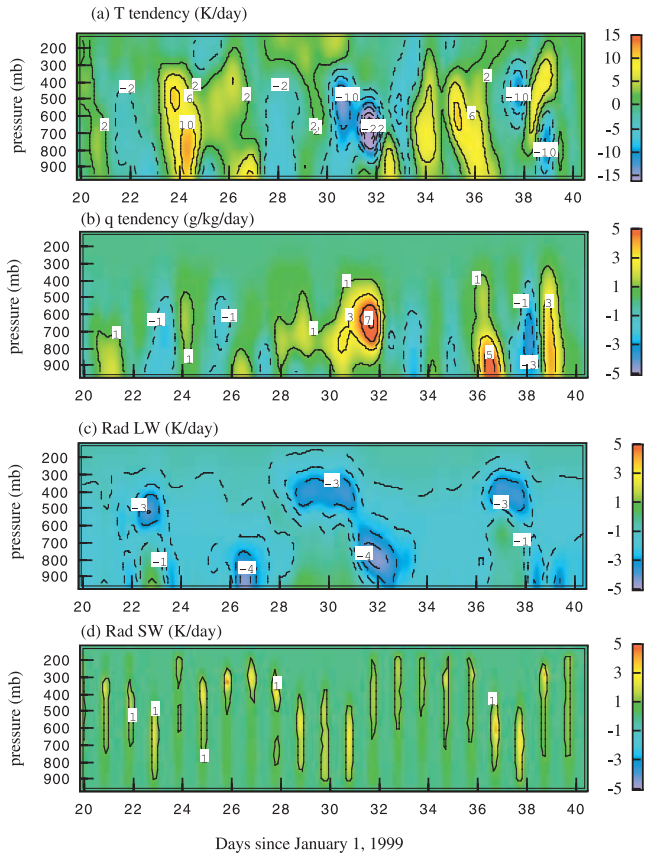

Figure 2. Temperature and water vapor tendencies derived from the ARM SGP winter 1999 IOP. (a) Advective and expansive temperature tendency. (b) Advective water vapor tendency. (c) and (d) Longwave and shortwave radiative cooling/heating rates.

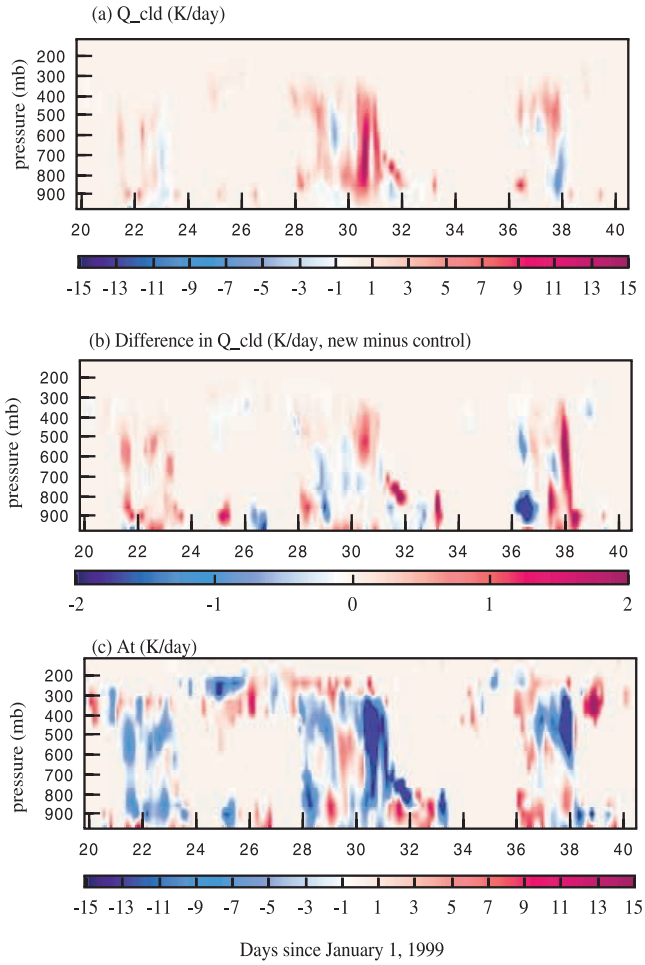

Figure 3. (a) Diagnosed condensational heating for the cloudy portion of the SGP with the new scheme ($\hat{Q}$). (b) Difference between the new scheme and the RK98 scheme. (c) Total temperature tendency from advection, expansion, and radiation.

Eliminating $\frac{\partial \hat{l}}{\partial t}$ between equations (17) and (18), one derives a prognostic equation of cloudiness as

$$\left[F_a^{-1} + \gamma \hat{l}^* \delta\right] \frac{\partial a}{\partial t} = \alpha \frac{\partial r}{\partial t} - \gamma a \delta \frac{\partial \hat{r}}{\partial t} - \left(\beta - \gamma a q_s'\right) \frac{\partial T_l}{\partial t} + F_b, \quad (19)$$

where $\delta = \left(1 + \frac{aLq_s'}{C_p}\right)^{-1} \cdot \frac{\partial \hat{r}}{\partial t}$ can be calculated from A_r and $\hat{R}_l$ following equation (14) written for cloudy portion of the grid box. Equation (19) is equivalent to equation (13). Once is $\frac{\partial a}{\partial t}$ known, $\frac{\partial \hat{l}}{\partial t}$ and $\frac{\partial l}{\partial t}$ can be determined, which can then be used to derive Q from equation (3).

3. Comparison With Other Schemes

[25] RK98 used two closure assumptions in its prognostic cloud scheme. The first was to derive the condensation rate for the cloudy part of the grid box. In the present notation, with the pressure tendency term neglected, this is given as (equation 10 of RK98):

$$Q_{cloudy} = a\left(\frac{\alpha \hat{A}_q - a\beta \hat{A}_T}{\alpha + a\frac{L}{Cp}\beta}\right). \quad (20)$$

In our formulation of section 2.1, this quantity is derived in equation (7) as

$$Q_{cloudy} = a\hat{Q} = a\left(\frac{\alpha \hat{A}_q - \hat{\beta} \hat{A}_T}{\hat{\gamma}}\right) = a\left(\frac{\alpha \hat{A}_q - \hat{\beta} \hat{A}_T}{\alpha + \frac{L}{Cp}\hat{\beta}}\right). \quad (21)$$

The difference between equations (20) and (21) is between the terms involving β. When a is equal to 1, they give the same results. When a equals to 0, the values within the parentheses can differ a lot, but since they are multiplied by a, the two formula also give the same results. When a is fractional, assuming that α is much larger than the β term in the denominators as is the case in the upper troposphere, the values of the denominators in the above equations are similar. Since $\hat{\beta} > a\beta$, a negative A_T is associated with a smaller Q_{cloudy} in equation (20). Because clouds are typically associated with negative A_T, caused by adiabatic cooling from upward motions, we expect RK98 to give smaller Q than the new formulation.

[26] RK98 used their second closure assumption to derive Q in the clear portion of the grid box, which is associated with the expansion and erosion of clouds. With notation in the current paper, equation (13) in RK98 is written as

$$Q_{clear} = \left(\frac{\hat{l}}{1 + a\frac{L}{Cp}\frac{\partial q_s}{\partial T}}\right)\frac{\partial a}{\partial t}. \quad (22)$$

Note that in RK98, $\frac{\partial a}{\partial t}$ is obtained from a previous time step, rather than from calculation coupled with Q. In the present

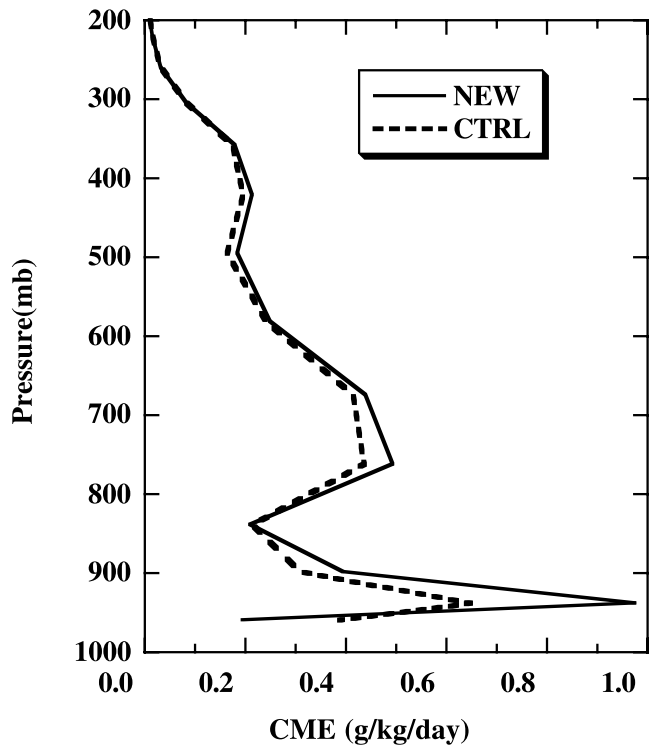

Figure 4. Stratiform condensation rate from using the new scheme (solid line) and from using the RK98 scheme (dashed line).

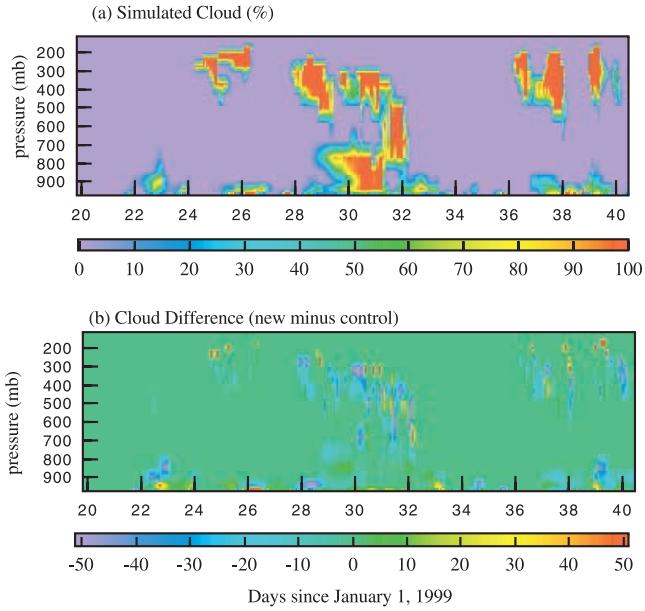

Figure 5. (a) Simulated cloud amount in the SCM with the new scheme. (b) Difference in clouds between the new scheme and the RK98 scheme.

formulation, this term Q_{clear} is not explicitly calculated, but it can be easily diagnosed as

$$Q_{clear} = Q - a\hat{Q}. \tag{23}$$

Using equations (21) and (23), equation (8) can be rewritten as

$$Q_{clear} = \hat{l}^* \frac{\partial a}{\partial t} - (1-a)A_l, \tag{24}$$

one can directly compare it with equation (22). Equation (24) states that the expansion and erosion of clouds are associated with both the condensation rate and the cloud water source in the clear-sky portion of the grid cell. Cloud can expand or erode simply due to horizontal advection or detrainment of water from convection. Even if $A_l = 0$, equation (24) differs from equation (22) in the coefficient of cloud change.

[27] In the formulation of S78 and *Sundqvist et al.* [1989], a closure equation was intuitively derived by assuming that the effect of the clear-sky portion of A_q and A_T, together with the evaporation of condensate, is balanced by the increase of clear-sky humidity and cloudiness. In the present notation, in the work by *Sundqvist et al.* [1989, equation (3.19)], it is written as

$$(1-a)\frac{\partial q_0}{\partial t} + \left(\hat{l} + q_s - q_0\right)\frac{\partial a}{\partial t} = (1-a)\left(A_q - \frac{\beta}{\alpha}A_T\right) + E_r, \tag{25}$$

where q_0 is the clear-sky mixing ratio, expressed as and $q_0 = q_s U_0$ and U_0 is a function of a described before. To make a contrast with the present formulation, we write the total water equation (14) for the cloudy portion of the grid box as

$$\frac{\partial \hat{r}}{\partial t} = \hat{A}_q + \hat{A}_l - \hat{R}_l. \tag{26}$$

Substituting the following

$$r = a\hat{r} + (1-a)q_0$$

into equation (14), and making use of equation (26), together with $R_l = a\hat{R}_l$, one gets

$$(1-a)\frac{\partial q_0}{\partial t} + (\hat{l} + q_s - q_0)\frac{\partial a}{\partial t} = (1-a)(A_q + A_l) + E_r. \tag{27}$$

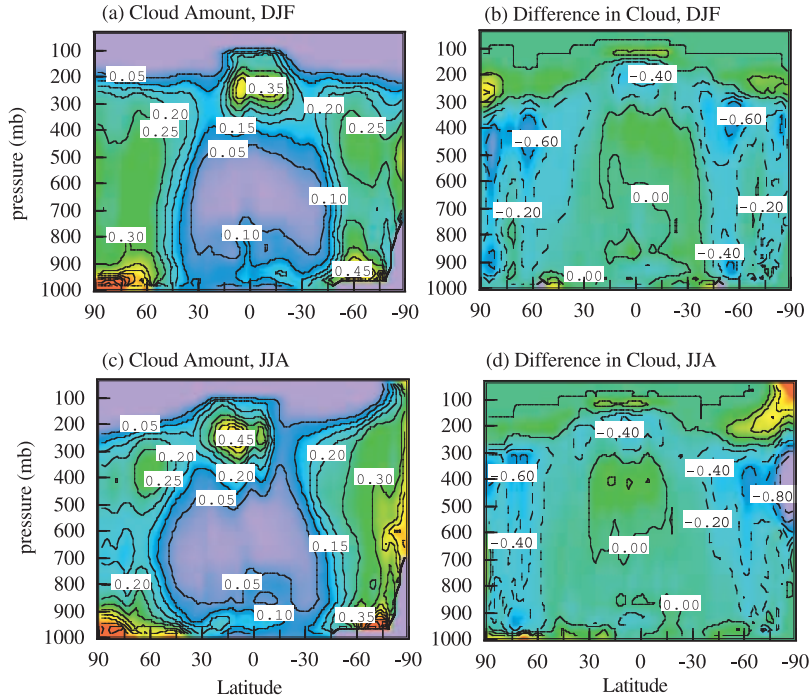

Figure 6. (a) Simulated cloud amount in the CCM with the new scheme in DJF. (b) Difference in clouds between the new scheme and the RK98 scheme in DJF. (c) and (d) Same as Figures 6a and 6b except for JJA.

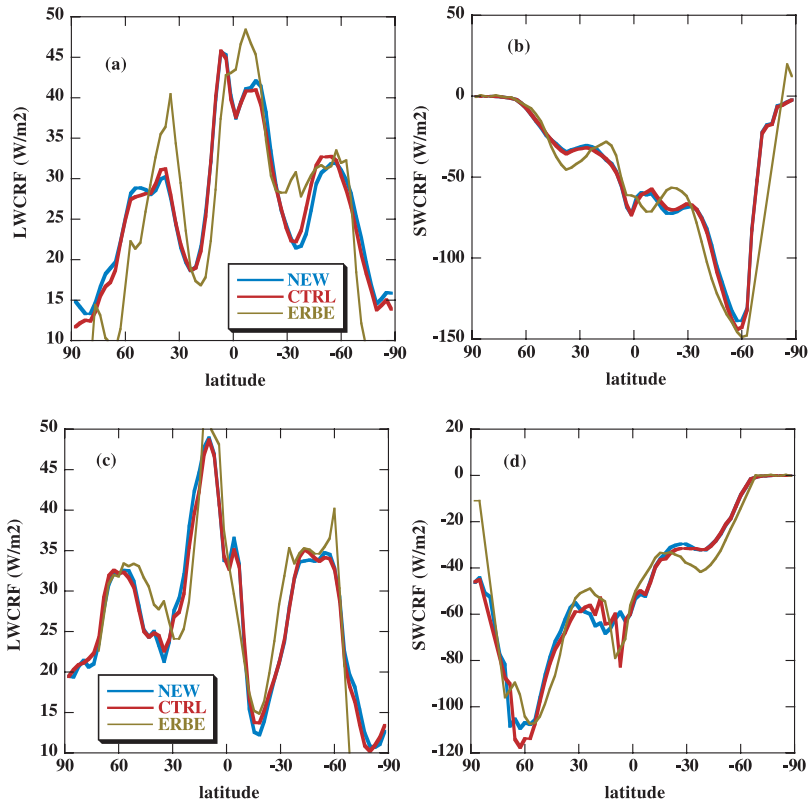

Figure 7. (a) Longwave cloud radiative forcing at the top of atmosphere in DJF. (b) Same as Figure 7a but for shortwave. (c) Same as Figure 7a but for JJA. (d) Shortwave for JJA.

[28] Comparing this with equation (25), it is seen that equation (25) does not include the term A_l, but it contains an extra term of A_T in the total water budget equation.

4. Impact on Model Results

[29] We first use field measurements from the Atmospheric Radiation Measurement (ARM) program at the Southern Great Plain (SGP) to analyze the differences. We choose the winter Intensive Observation Period (IOP) of 1999 to minimize the impact of convection. Figure 1 shows the time-pressure cross sections of the temperature, water vapor mixing ratio, and the observed cloud frequency at the ARM SGP central facility [*Clothiaux et al. 2001*]. Figures 2a and 2b show the advective and expansion tendencies of temperature and water vapor mixing ratio analyzed from the SGP sounding network by using the constrained variational analysis of *Zhang et al.* [2001]. Negative advective/expansion temperature tendency is generally associated with positive water vapor tendency. Two main events occurred around day 31 and day 38. Even though three synoptic cloud events are seen in Figure 1c, the first one is associated with little precipitation. Note that the cloud field is from a single station, while the advective tendency fields are analyzed for a domain of about 300 km in radius. Therefore, the observations are shown only to gain insight about the range of scheme differences.

[30] We further estimated the rate of longwave radiative cooling and shortwave heating for this period as shown in Figures 2c and 2d. They are calculated by using the CCM3 radiation code with observed temperature, water vapor and cloud mask profiles in Figure 1. Cloud liquid water and ice water concentrations are estimated by using the CCM3 diagnostic parameterization with the total liquid water path constrained to the ARM microwave radiometer measurements.

[31] Figure 3a shows the calculation of the condensational heating rate $\hat{Q}$ of the cloudy portion of the grid by using the above tendencies as input. Figure 3b shows the difference between the present scheme in section 2.1 and RK98. It is seen that the large-scale condensation is generally systematically larger in the present calculation, by about ten percent. The pattern of the difference distribution can be clearly explained by examining the pattern of the total temperature tendency masked by clear sky shown in Figure 3c: negative temperature tendency is associated with larger heating rate in the present formulation.

[32] Because we do not have measurements of the vertical distribution of cloud water concentration, we cannot easily evaluate other aspects of the impact of the scheme. We therefore use the NCAR CCM Single Column Model (SCM) (see J. J. Hack et al.'s *SCCM User*'s *Guide* available at http://www.cgd.ucar.edu/cms/sccm/sccm.html) and force the SCM by using the advective tendencies in Figures 2a and 2b. Figure 4 shows the time averaged vertical profiles of the stratiform condensation rate from using the present scheme and the RK98 scheme. Consistent with the diagnostic calculation, the present scheme gives systematically larger condensational heating rate when there is fractional cloud coverage.

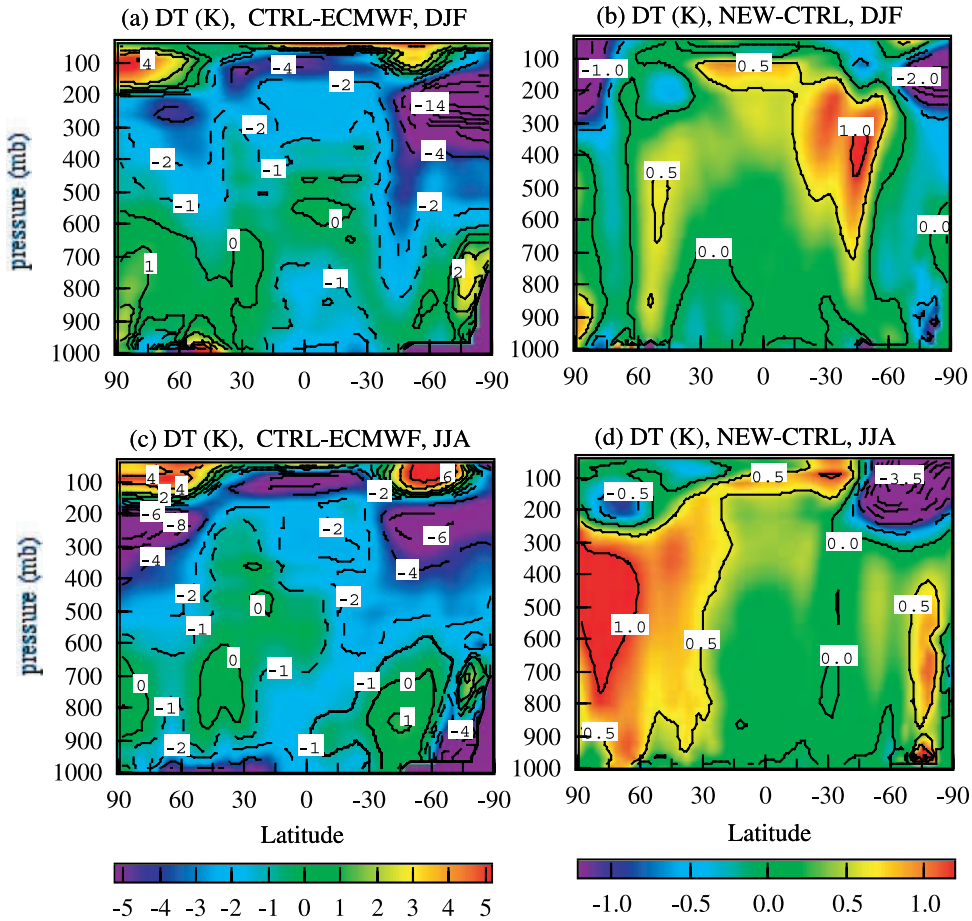

Figure 8. (a) Temperature bias in the CCM simulation using RK98 for DJF relative to ECMWF reanalysis. (b) Temperature difference between the new scheme and RK98 for DJF. (c) and (d) Same as Figures 7a and 7b except for JJA.

[33] Figure 5a shows the simulation of clouds in the SCM with the new formulation. Comparing with observed cloud frequency in Figure 1c, the first event is completely missed possibly because the SCM does not include hydrometer advection. The other two events are simulated with some success even though the SCM contains large biases in temperature and moisture similar to those shown by *Hack and Pedretti* [2000] and *Xie and Zhang* [2000]. Figure 5b shows the difference in clouds relative to the simulation by using RK98. As expected, the direct impact of a larger condensation rate is a warmer and drier upper atmosphere and fewer clouds.

[34] We then use the above diagnostic and SCM results to interpret the impact of the scheme on GCM results. The NCAR CCM3 is integrated for five years by using the new scheme and the RK98 scheme with climatological seasonal SST forcing. The general features of the model simulation using the RK98 are essentially identical to those presented in RK98. Figures 6a and 6b show the distribution of simulated cloud amount with the new scheme, and its change relative to the RK98 simulation in the northern winter season. Figures 6c and 6d show the corresponding figures in the northern summer. As expected, the new scheme results in an overall reduction in clouds in the middle and upper troposphere.

[35] The reduction in cloudiness corresponds to appreciable changes in cloud radiative forcing (CRF), especially in the longwave. We therefore reduced the autoconversion of cold cloud ice to snow in the RK98 microphysical package by changing the threshold value of the ice-mixing ratio. In RK98, autoconversion of ice to snow takes place when the ice mixing ratio exceeds a threshold which is a ramp function of temperature with value of 4×10^{-4} at T = 0°C and 5×10^{-6} at T = −20°C. In the actual implementation within CCM3, the latter was reduced to 4×10^{-6}. We raised it to 6×10^{-6}. This tuning is a result of the crude parameterization of the clouds and its microphysics in the model. This resulted in more cloud ice water in the model to offset the reduced cloudiness in making up the radiative budget of the original model. Figures 7a and 7b show the zonally averaged cloud radiative forcing at the top of the atmosphere, separately for longwave and shortwave for the northern winter season. Also plotted is the satellite measurement from the Earth Radiation Budget Experiment (ERBE). Figures 7c and 7d show the corresponding figures for the northern summer season. It is seen that the overall change between simulations using the new scheme and RK98 is negligible, much smaller than the difference between the model results and the measurements.

[36] The zonal averaged climate simulated using the original CCM with RK98 contains an overall cold bias in the upper troposphere relative to the ECMWF reanalysis, as shown in Figure 8a for DJF and Figure 8c for JJA. This is

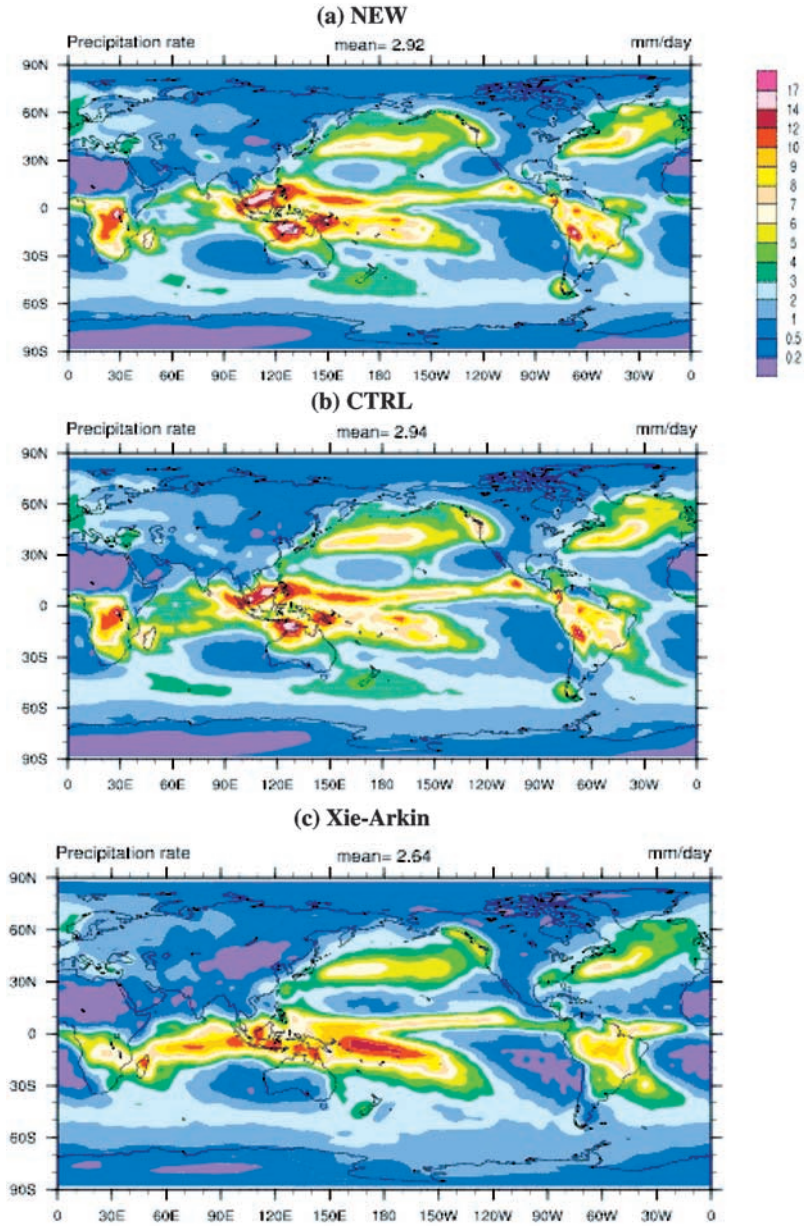

Figure 9. Simulated and observed precipitation for the DJF season. (a) New scheme, (b) RK98 scheme, (c) Xie and Arkin analysis.

also true when the NCEP/NCAR reanalysis is used as reference (not shown). Figures 8b and 8c show the change of temperature simulated with the new scheme relative to that with RK98. It is seen that the present formulation gives a slight broad warming in the troposphere, toward reducing the original cold bias. We have performed several other 5-year model runs starting with different initial conditions and this feature remains to be statistically significant.

[37] Other aspects of the simulated model climate are very close to the control simulation by using the RK98 scheme. As an example, Figure 9 shows the DJF seasonal averaged distribution of precipitation from using the new scheme, the RK98 scheme, and from the *Xie and Arkin* [1997] analysis. It is seen that difference of precipitation between the schemes is much smaller than those between models and observation. This insensitivity of the model climate to the prognostic cloud scheme is consistent with RK98 who also reported relatively small difference in climate between the prognostic and diagnostic cloud schemes. This is not entirely unexpected since all these simulations used the same subgrid-scale assumption (9). Other aspects of the model simulations are therefore not presented. The merit of the improved formulation, however, is in the physical consistencies of the calculation, which would allow us to incorporate more robust subgrid and microphysical physics.

5. Summary

[38] We have described modifications to the *Rasch and Kristjànsson* [1998] prognostic cloud scheme. The main point is to link the cloudiness change with variation of the

total condensate. This is facilitated by the introduction of an in-cloud condensate equation. This link, together with the diagnostic cloud scheme, forms a closure to calculate the fractional condensate rate. As a result, the new formulation eliminates the two closure assumptions in the original model. We have made comparisons of the present formulation with other schemes. Calculation is made relative to RK98 by using ARM measurements and using the NCAR CCM. It was shown that the present scheme gives slightly larger condensational heating, less clouds, and a warmer troposphere.

[39] Much remains to be done to improve the present formulation and its CAM2 implementation. The formulation in section 2.4 should be implemented and tested in CAM2. The number of hydrometer species should be increased. The same procedure of section 2 can be used if ice and water clouds are separately considered. Another important aspect is the incorporation of more realistic subgrid-scale features to replace the diagnostic cloud relationship of equation (9), in particular, when convection is present.

[40] **Acknowledgments.** This research is supported by the Atmospheric Radiation Program of the Department of Energy under grant EFG0298ER62570, and by NSF under grant ATM901950, to the State University at Stony Brook. NCAR is sponsored by the National Science Foundation. We thank Moguo Sun for valuable discussions at the early stage of this work, David Randall for informing us of his recent research on the next generation cloud parameterization in the CSU GCM. We thank the two anonymous reviewers whose comments have led to large improvement of the original paper.

References

Arakawa, A., and W. H. Schubert, Interaction of a cumulus cloud ensemble with the large-scale environment Part I, *J. Atmos. Sci.*, *31*, 674–701, 1974.

Cess, R. D., et al., Intercomparison and interpretation of climate feedback processes in 19 atmospheric general circulation models, *J. Geophys. Res.*, *95*, 16,601–16,615, 1990.

Clothiaux, E. E., et al., The ARM Millimeter Wave Cloud Radars (MMCRs) and the Active Remote Sensing of Clouds (ARSCL) Value Added Product (VAP), 56 pp., *DOE Tech. Memo. ARM VAP-002.1*, 2001.

Cubasch, U., Climate change 2001: The scientific basis, in *Contribution of Working Group I to the Third Assessment Report of the Intergovernmental Panel on Climate Change*, pp. 528–582, Cambridge Univ. Press, New York, 2001.

Del Genio, A., M.-S. Yao, W. Kovari, and L. W. Lo, A prognostic cloud water parameterization for global climate models, *J. Clim.*, *9*, 270–304, 1996.

Fowler, L., D. A. Randall, and S. A. Rutledge, Liquid and ice cloud microphysics in the CSU general circulation model, I, Model description simulated microphysical processes, *J. Clim.*, *9*, 489–529, 1996.

Ghan, S. J., and R. C. Easter, Computationally efficient approximations to stratiform cloud microphysics parameterization, *Mon. Weather Rev.*, *120*, 1572–1582, 1992.

Hack, J. J., and J. A. Pedretti, Assessment of solution uncertainties in single-column model frameworks, *J. Clim.*, *13*, 352–356, 2000.

Kiehl, J. T., J. J. Hack, G. B. Bonan, B. A. Boville, B. P. Briegleb, D. L. Williamson, and P. J. Rasch, Description of the NCAR Community Climate Model (CCM3), *NCAR Tech. Note NCAR/TN-420+STR*, 151 pp., Natl. Cent. for Atmos. Res., Boulder, Colo., 1996.

Le Treut, H., and Z. X. Li, Using Meteosat data to validate a prognostic cloud water scheme, *Atmos. Res.*, *21*, 273–292, 1988.

Mitchell, J. F. B., and W. J. Ingram, Carbon dioxide and climate: Mechanisms of changes in cloud, *J. Clim.*, *5*, 5–21, 1992.

Randall, D. A., and L. D. Fowler, Eauliq: The next generation, *Atmos. Sci. Pap. 673*, 65 pp., Colo. State Univ., Boulder, Colo., 2001.

Rasch, P. J., and J. E. Kristjànsson, A comparison of the CCM3 model climate using diagnosed and predicted condensate parameterizations, *J. Clim.*, *11*, 1587–1614, 1998.

Slingo, J. M., The development and verification of a cloud prediction scheme for the ECMWF model, *Q. J. R. Meteorol. Soc.*, *113*, 899–927, 1987.

Smith, R. N. B., A scheme for predicting layer clouds and their water content in a general circulation model, *Q. J. R. Meteorol. Soc.*, *116*, 435–460, 1990.

Somerville, R. C. J., and L. A. Remer, Cloud optical thickness feedbacks in the CO2 climate problem, *J. Geophys. Res.*, *89*, 9668–9672, 1984.

Sundqvist, H., A parameterization scheme for nonconvective condensation including prediction of cloud water content, *Q. J. R. Meteorol. Soc.*, *104*, 677–690, 1978.

Sundqvist, H., E. Berge, and J. E. Kristjànsson, Condensation and cloud parameterization studies with a mesoscale numerical weather prediction model, *Mon. Weather Rev.*, *117*, 1641–1657, 1989.

Tiedtke, M., Representation of clouds in large-scale models, *Mon. Weather Rev.*, *121*, 3040–3061, 1993.

Xie, P., and P. A. Arkin, Global precipitation: A 17-year monthly analysis based on gauge observations, satellite estimates, and numerical model outputs, *Bull. Am. Meteorol. Soc.*, *78*(11), 2539–2558, 1997.

Xie, S. C., and M. H. Zhang, Impact of the convection triggering function on single-column model simulations, *J. Geophys. Res.*, *105*, 14,983–14,996, 2000.

Zhang, G. J., and N. A. McFarlane, Sensitivity of climate simulations to the parameterization of cumulus convection in the Canadian Climate Centre general circulation model, *Atmos. Ocean*, *33*, 407–446, 1995.

Zhang, M. H., J. L. Lin, R. T. Cederwall, J. J. Yio, and S. C. Xie, Objective analysis of the ARM IOP data: method and sensitivity, *Mon. Weather Rev.*, *129*, 295–311, 2001.

Zhao, Q., T. L. Black, and M. E. Baldwin, Implementation of the cloud prediction Scheme in the Eta Model at NCEP, *Weather Forecast.*, *12*(3), 697–712, 1997.

C. S. Bretherton, Department of Atmospheric Sciences, 710 ATG, University of Washington, Seattle, WA, 98195, USA. (breth@atmos.washington.edu)

J. Hack and P. Rasch, NCAR, Boulder, CO, 80305, USA. (jhack@ucar.edu; pjr@ucar.edu)

W. Lin and M. H. Zhang, ITPA/MSRC, State University of New York, Stony Brook, NY, 11794-5000, USA. (wlin@atmsci.msrc.sunysb.edu; mzhang@notes.cc.sunysb.edu)